

PPPL- 5035

PPPL- 5035

Understanding Ion Cyclotron Harmonic Fast Wave Heating Losses in the Scrape Off Layer of Tokamak Plasmas

N. Bertelli, E.F. Jaeger, J.C. Hosea, C.K. Phillips, L. Berry, P.T. Bonoli,
S.P. Gerhardt, D. Green, B. LeBlanc, R.J. Perkins, P.M. Ryan, G. Taylor¹,
E.J. Valeo, J.R. Wilson and J.C. Wright

June 2014



Princeton Plasma Physics Laboratory

Report Disclaimers

Full Legal Disclaimer

This report was prepared as an account of work sponsored by an agency of the United States Government. Neither the United States Government nor any agency thereof, nor any of their employees, nor any of their contractors, subcontractors or their employees, makes any warranty, express or implied, or assumes any legal liability or responsibility for the accuracy, completeness, or any third party's use or the results of such use of any information, apparatus, product, or process disclosed, or represents that its use would not infringe privately owned rights. Reference herein to any specific commercial product, process, or service by trade name, trademark, manufacturer, or otherwise, does not necessarily constitute or imply its endorsement, recommendation, or favoring by the United States Government or any agency thereof or its contractors or subcontractors. The views and opinions of authors expressed herein do not necessarily state or reflect those of the United States Government or any agency thereof.

Trademark Disclaimer

Reference herein to any specific commercial product, process, or service by trade name, trademark, manufacturer, or otherwise, does not necessarily constitute or imply its endorsement, recommendation, or favoring by the United States Government or any agency thereof or its contractors or subcontractors.

PPPL Report Availability

Princeton Plasma Physics Laboratory:

<http://www.pppl.gov/techreports.cfm>

Office of Scientific and Technical Information (OSTI):

<http://www.osti.gov/bridge>

Related Links:

[U.S. Department of Energy](#)

[Office of Scientific and Technical Information](#)

[Fusion Links](#)

Understanding ion cyclotron harmonic fast wave heating losses in the scrape off layer of tokamak plasmas

N. Bertelli¹, E. F. Jaeger², J. C. Hosea¹, C. K. Phillips¹, L. Berry³, P. T. Bonoli⁴,
S. P. Gerhardt¹, D. Green³, B. LeBlanc¹, R. J. Perkins¹, P. M. Ryan³, G. Taylor¹, E. J. Valeo¹,
J. R. Wilson¹ and J. C. Wright⁴

¹ Princeton Plasma Physics Laboratory, Princeton, NJ 08543, USA

² XCEL Engineering Inc., Oak Ridge, TN 37830, USA

³ Oak Ridge National Laboratory, Oak Ridge, TN 37831-6169, USA

⁴ Plasma Science and Fusion Center, MIT, Cambridge, MA 02139, USA

Introduction. Fast waves at harmonics of the ion cyclotron frequency, which have been used successfully on National Spherical Torus Experiment (NSTX) [1], will also play an important role in ITER and are a promising candidate for the Fusion Nuclear Science Facility (FNSF) designs based on spherical torus (ST) [2]. Experimental studies of high harmonic fast waves (HHFW) heating on the NSTX have demonstrated that substantial HHFW power loss occurs along the open field lines in the scrape-off layer (SOL), but the mechanism behind the loss is not yet understood [3, 4, 5, 6, 7]. The full wave RF code AORSA [8], in which the edge plasma beyond the last closed flux surface (LCFS) is included in the solution domain [9], is applied to specific NSTX discharges in order to predict the effects and possible causes of this power loss. In the studies discussed here, a collisional damping parameter has been implemented in AORSA as a proxy to represent the real, and most likely nonlinear, damping processes [10]. A prediction for the NSTX Upgrade (NSTX-U) experiment, that will begin operation next year, is also presented, indicating a favorable condition for the experiment due to a wider evanescent region in edge density.

Numerical results. Figure 1 shows the wave electric field amplitude obtained by the 2D full wave code AORSA for a single (dominant) toroidal mode, $n_\phi = -21$, corresponding to an antenna phase of -150° in (a) and for $n_\phi = -12$, corresponding to an antenna phase of -90° , in (b), for NSTX discharge 130608 [5, 9, 11]. The wave frequency is $f = 30$ MHz. Six different cases of the electron density, n_{ant} , in front of the antenna (indicated in white) are plotted for both antenna phases, together with the contour (in white) corresponding to the right hand cut-off in the cold plasma approximation [12]. In Figure 1, the black curves indicate the LCFS. This figure clearly shows that as soon as the density in front of the antenna increases sufficiently to "open" the FW cut-off in front of the antenna, the wave electric field amplitude in the SOL increases strongly. In other words, these simulations show a strong correlation between the location of

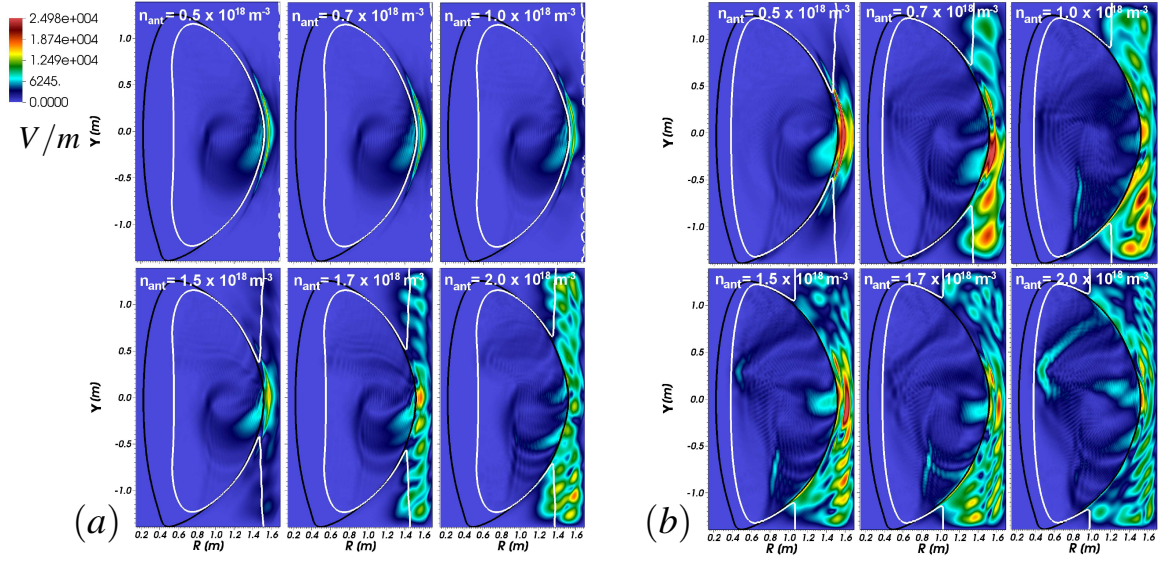


Figure 1: Electric field amplitude for different density values in front of the antenna (n_{ant}) (shown in the plots) with toroidal mode numbers $n_{\phi} = -21$ (a) and $n_{\phi} = -12$ (b). The white and black curves indicate the FW cut-off layer and the last closed flux surface, respectively.

the FW cut-off layer with the large electric field amplitude. When the FWs are no longer cut-off in front of the antenna and are instead propagating, the electric field amplitude outside of the LCFS increases. When the FW cut-off is “closed” in front of the antenna and the waves are evanescent, the RF field amplitude in the SOL remains small. For very low density, the RF field is strongly peaked radially and localized in front of the antenna, because the wave is strongly evanescent. For high density, when the wave is propagating, standing waves appear to form outside of LCFS independent of the launched wavenumber selected (see also [9, 11]). In fact, these results appear for both antenna phases shown. Furthermore, it appears that with increasing density, the RF field amplitude in the SOL increases but not monotonically. The above effects are more evident for $n_{\phi} = -12$ (Figure 1(b)). In the simulations shown in Figure 1, no SOL power losses are found, even though the “standard” kinetic effects (Landau damping and transit-time magnetic pumping) are retained in the hot plasma dielectric tensor throughout the entire plasma.

Figure 2(a) shows the predicted absorbed power in the SOL region (SOL power losses) as a function of the density in front of the antenna (n_{ant}) assuming $\nu/\omega = 0.01$, where ν is the collision frequency and ω is the angular wave frequency. Two different antenna phases are shown: $n_{\phi} = -12$ (dashed curve) and -21 (solid curve). The cut-off of the fast wave corresponds to the right hand cut-off, which for a single ion species plasma and $\omega < |\omega_{\text{ce}}|$, can be

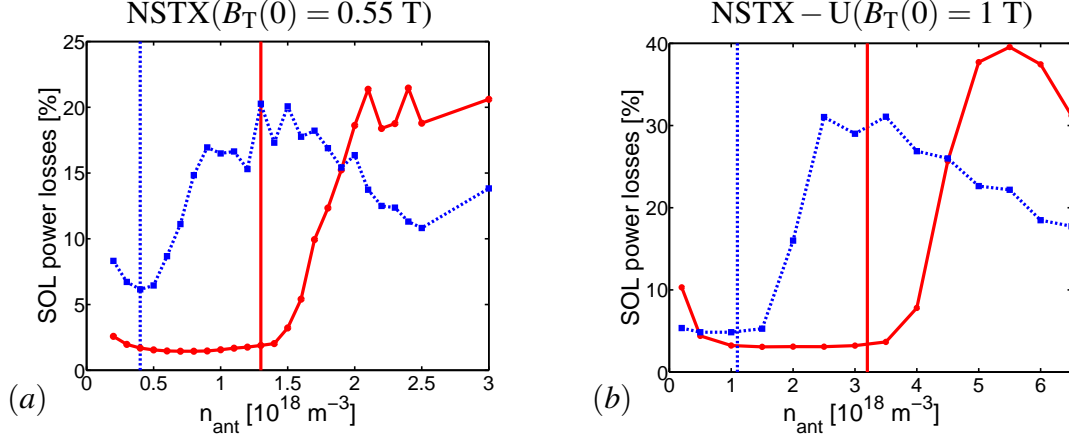


Figure 2: Fraction of power lost to the SOL as a function of the density in front of the antenna for $n_\phi = -21$ (solid curve) and $n_\phi = -12$ (dashed curve), for an NSTX case with $B_T = 0.55$ T (fig. (a)) and an NSTX-U case with $B_T(0) = 1$ T (fig. (b)). The vertical lines represent the value of the density for which the FW cut-off starts to be “open” in front of the antenna (see Fig. 1).

written as [3, 4]

$$n_{e,\text{FWcut-off}} \propto \frac{k_{\parallel}^2 B}{\omega}, \quad (1)$$

where ω_{ce} is the electron gyrofrequency, k_{\parallel} is the parallel (to the magnetic field) component of the wave vector, and B is the equilibrium magnetic field. The vertical line in Figure 2(a), for both cases, represents the density at which the cut-off starts to be “open” in front of the antenna, i.e., when the wave is propagating in front of the antenna and the amplitude of the electric field starts to increase in the SOL region, as shown in Figure 1. From Figure 2(a) one can note a rapid transition in the fraction of the power lost to the SOL from the evanescent region to the propagating region both for $n_\phi = -12$ and -21 . Moreover, for lower n_ϕ ($n_\phi/R = k_\phi \sim k_{\parallel}$) the transition occurs at lower n_{ant} as expected from Eq.1. When the cut-off is “closed” in front of the antenna and the wave is evanescent, with a small SOL RF field amplitude, the fraction of power lost to the SOL is found to be smaller with respect to the regime in which the cut-off is “open” and the wave propagating in the SOL has a large RF field amplitude. For very low density the RF power losses tend to increase again with decreasing density, due to the fact that the wave is so strongly evanescent that the power can be only damped in front of the antenna, consistent with the large electric field localized in front of the antenna as indicated in Figure 1. This effect is more evident for the $n_\phi = -12$ than $n_\phi = -21$ because of the significant shift of the FW cut-off density toward lower density and, as a consequence, a narrower density range for the evanescent region. It is also important to mention that in the density range adopted in these simulations the slow wave is found to be cut-off.

We can now extend our numerical analysis to the NSTX-U experiment, which will be operating at the beginning of 2015 [13], in order to make some predictions on the behavior of the RF power losses in future NSTX-U discharges. We analyze an H-mode scenario being considered for NSTX-U with $B_T(0) = 1$ T, obtained by using the TRANSP code [14]. This toroidal magnetic field corresponds to the full toroidal magnetic field that will be available for the NSTX-U experiment. Figure 2(b) shows the predicted RF power losses in the SOL as a function of n_{ant} for this NSTX-U case. Exactly the same transition behavior found in the NSTX case is predicted for the NSTX-U case for both $n_\phi = -21$ (solid curve) and $n_\phi = -12$ (dashed curve). The important difference is that the transition to higher losses in the SOL in NSTX-U at $B_T(0) = 1$ T occurs at higher density than in NSTX at $B_T(0) = 0.55$ T. This is explained by the fact that the FW cut-off is proportional to the magnetic field (see Eq. 1) (compare vertical lines in Figures 2(a) and 2(b) for each n_ϕ). This result tells us that the evanescent region for NSTX-U, in which the SOL power losses are smaller, will be wider than the one in NSTX and therefore from the experimental point of view there will be a wider SOL density range in which the experiment can run with lower SOL power losses [11].

This work was supported by the SciDAC Center for Wave-Plasma Interactions under DE-FC02-01ER54648 and the US DOE under DE-AC02-CH0911466.

References

- [1] M. Ono et al., *Nucl. Fusion* **40**, 557 (2000)
- [2] Peng Y.-K.M. et al, *Plasma Phys. Control. Fusion* **47**, B263 (2005)
- [3] J. C. Hosea et al., *Phys. Plasmas* **15**, 056104 (2008)
- [4] C. K. Phillips et al., *Nucl. Fusion* **49**, 075015 (2009)
- [5] G. Taylor et al., *Phys. Plasmas* **17**, 056114 (2010)
- [6] R. J. Perkins et al., *Phys. Rev. Lett.* **109**, 045001 (2012)
- [7] R. J. Perkins et al., *Nucl. Fusion* **53**, 083025 (2013)
- [8] E. F. Jaeger et al., *Phys. Plasmas* **8**, 1573 (2001)
- [9] D. L. Green et al., *Phys. Rev. Lett.* **107**, 145001 (2011)
- [10] N. Bertelli et al., *AIP Conf. Proc.* **1580**, 310 (2014)
- [11] N. Bertelli et al., *Nucl. Fusion* **54**, 083004 (2014)
- [12] T. H. Stix, *Waves in Plasmas*, American Institute of Physics, NY, (1992)
- [13] J. E. Menard et al., *Nucl. Fusion* **52**, 083015 (2012)
- [14] S. P. Gerhardt, R. Andre, and J. E. Menard, *Nucl. Fusion* **52**, 083020 (2012)

The Princeton Plasma Physics Laboratory is operated
by Princeton University under contract
with the U.S. Department of Energy.

Information Services
Princeton Plasma Physics Laboratory
P.O. Box 451
Princeton, NJ 08543

Phone: 609-243-2245
Fax: 609-243-2751
e-mail: pppl_info@pppl.gov
Internet Address: <http://www.pppl.gov>